PFC/JA-95-2

The Visible, Imaging Diode Arrays on Alcator C-Mod

J.L. Terry, J.A. Snipes, C. Kurz

January, 1995

Submitted to Rev. Sci. Instrum.

This work was supported by the U. S. Department of Energy Contract No. DE-AC02-78ET51013. Reproduction, translation, publication, use and disposal, in whole or in part by or for the United States government is permitted.

The following will be published in Rev. Sci. Instrum. , Vol. 66, No. 1, January 1995

The Visible, Imaging Diode Arrays on Alcator C-Mod

J.L. Terry, J.A. Snipes, and C. Kurz
MIT Plasma Fusion Center
Cambridge, Massachusetts 02139
USA

Abstract

A set of multi-chord, absolutely calibrated viewing arrays has been used to measure the distributions of H/D and C^{+2} emissions. A total of 227 chordal views are available, with the chords separated at the plasma by ~1 cm typically. The chord brightness profiles have been combined and inverted (without recourse to symmetry assumptions) to yield local volume emission rates. Because of the thickness of the superstructure surrounding Alcator C-Mod, the views are from points re-entrant to the vacuum vessel. All but one of the arrays employ 64-channel, linear diode arrays, which are read out serially, thus requiring only one digitizer channel per array. Variable frame rates (~1 Hz to ~3.5 kHz) result in an extremely large dynamic range for these detectors. A 35-channel diode array which is read out in parallel and can track fast events like ELMs or pellets is also in use.

Introduction

The lower temperature plasmas in the divertors and scrape-off layers of present-day tokamaks are under intense investigation due to the difficulty of achieving acceptable heat removal from a burning, ITER plasma. It is advantageous for the temperature in the divertor to be low, so that a significant fraction of the power flowing into the scrape-off layer can be radiated before it is conducted to the divertor plate, and so that sputtering thresholds are not exceeded. Low divertor T_e also allows for the existence of a partially ionized plasma in which parallel ion momentum can be absorbed[1]. The visible radiation from hydrogen and intrinsic or seeded impurities, emitted under these conditions, can serve as a valuable diagnostic[2,3] for this plasma. However, the emissions from the divertor and scrape-off layer typically have complicated spatial distributions. This is a result of the absence of poloidal symmetry in the magnetic geometry ('dee' shaped cross-sections and poloidal divertors) and the presence of localized plasma phenomena (e.g. MARFEs, radiative divertors). On Alcator C-Mod (which has both a shaped plasma cross-section and a poloidal divertor)[4] a number of flexible, low-cost visible imaging systems that view the plasma and internal vessel structures through visible interference filters are in use. The purpose of these spatially resolving arrays is to provide absolute brightness measurements along many different chords which can be inverted in a way such that *local* intensities can be determined.

Description of the Arrays and Their Views

One of the diode arrays, which views the discharge from above, contains 35 elements, each 0.9x4.4 mm^2 in size. The signal from each diode is amplified and digitized separately, and as such differs only in its use of a lens and interference filter from the x-ray arrays which have been standard on fusion devices for many years[5]. The filter, lens, and array are placed behind the window at the end of a re-entrant tube. The 35 chordal views are spaced equally within the fan labeled 'Top Array #1' in Figure 1. The entire field-of-view in a plane at the divertor is 0.47 m radially and 0.065 m toroidally. The parallel readout of this array allows observation of fast events (up to 1MHz) like ELMs and pellet ablation. It views the paths of the D_2 pellets injected into C-Mod.

The other visible arrays employ 64-channel Reticon[6] self-scanning, linear diode arrays. The desired sections of plasma are imaged (through windows on re-entrant tubes) onto 8x10 mm, coherent fiber bundles of lengths 1.8 or 4 m. The bundles have a resolution of 50 line pairs/mm, but do not transmit usefully below 400 nm, and are subject to transmission degradation if exposed to neutron or gamma radiation. The images transmitted by each bundle are viewed in two colors by employing a beamsplitter in front of two SLR camera lenses. Following each of these lenses is an interference filter and a lens which demagnifies the image onto the diode array. Thus for each view, two visible emission lines can be observed. The filters can be mounted in wheels and selected remotely. The individual diode elements are 0.05 mm x 2.5 mm rectangles. This and the choices of plasma-viewing-lens, bundle size, and demagnifying lenses determine the field-of-view in the plasma of each diode. Typically, for these arrays, adjacent chords are separated by ~1 cm in the plasma. If there is a significant toroidal curvature over the long dimension of the rectangular diode elements (the "toroidal" dimension in the plasma), then it should be masked to avoid loss of radial resolution. (See 'Results-Brightness Profiles' section.)

Two primary advantages are gained with the use of these devices. First, a very large dynamic range of measurable brightnesses is achieved by varying the length of time the diodes integrate the detected light (the frame time). Typical frame rates ranged from 0.05 to 1 kHz, although rates from ~1 Hz to ~3.5 kHz are possible. Independent of the integration time, the frame data are read out in 680 μs typically, although this interval can be reduced to 272μs. Brightnesses from ~0.1 to ~100 $W/m^2/ster$ have been measured routinely. Second, the time histories of a large number (64) of chordal brightnesses are acquired on a single digitizer channel. The three different plasma views of these arrays are shown in Figure 1 as 'Top Array #2' and 'Side Array #1' and '#2'.

All of the arrays in combination provide nearly full coverage of Alcator C-Mod's poloidal cross-section, missing only those regions shadowed by the closed divertor structures. The views are not all in the same toroidal section. 'Top Array #1' is displaced toroidally from 'Side Array #1' and 'Top Array #2' by 36°, and 'Side Array #2' is displaced an additional 108°. Thus the composite picture constructed from these views assumes toroidal symmetry in the emission.

Calibration of the Arrays

In order to use all the arrays in combination, the absolute sensitivity of each diode in each array (including all of the imaging optics) was measured. In addition, the view of each diode was determined. This was done in three steps.

First, the optical axis of each chordal view was measured relative to the C-Mod vacuum vessel. (In most cases this was done by moving a light source to known positions inside the vacuum vessel.) Second, the relative sensitivity of each view within a given array was calibrated. Although the responses of the diodes are quite uniform, the imposition of the imaging optics resulted in nonuniformities. It is also extremely desirable that the relative sensitivity for a given array be independent of the interference filter in front of it. To meet this condition, the filter bandpasses were made >2.5 nm (FWHM), so that the $\pm 6^{\circ}$ spread in the rays incident on the filter had a negligible effect on the transmission. Relative calibration was accomplished by moving a low pressure, H_2 lamp across the array field-of-view (with the array's H_{α}/D_{α} filter in place), and by making sure that the lamp image overfilled each individual diode. The independence of the relative calibration to the central wavelength of the filter was verified by doing the same with a He lamp and the array's HeI filter (λ_0=588 nm). Finally, the absolute sensitivity of a given diode's view within each array was measured using an absolutely calibrated tungsten ribbon lamp. Our estimate of the uncertainty in the absolute angular position of the arrays is $\sim 1^{\circ}$, while the uncertainty in the diode-to-diode sensitivity within an array is $\pm$ 10% and the uncertainty of the sensitivities among arrays is $\pm$ 20%.

Results - Brightness Profiles

In the tokamak environment the arrays have operated with low noise and no detectable RF pickup from the ICRF auxiliary heating (up to 1 MW of RF power). The accuracy of the calibrations is best illustrated by constructing profiles generated by arrays which have chords covering the same poloidal regions, but which are displaced toroidally. Such a profile of D_{α} emission, using radially inward views, is shown in Figure 2a. The profile is constructed from Side Array #1 and #2 (separated toroidally by 108°), and, along the common poloidal chords, the agreement in brightness is quite good. In Figure 2b is shown a radial profile of D_{α} emission, as seen from above, looking through the main plasma and into the divertor (Top Array #1 and #2, separated by 36° toroidally). The measured brightnesses over the common poloidal region agree only over part of the profile. Further investigation has revealed that the disagreement is a result of the wide toroidal field-of-view of Top Array #2. For these measurements, the array was used with its full toroidal view, and the field-of-view at the divertor of each of its diodes was an 80 cm (along a line tangent to a toroidal arc) x 1.6 cm (radial) rectangle, compared to a 6.5 x 1.33 cm^2 rectangle for a diode of Top Array #1. Thus the bright, radially narrow band of emission, seen by Array #1 at R_{maj} =0.68 m, will curve over and be averaged by almost 8 of the Top Array #2 diodes. This effect is seen in the Top #2 data, and since this limits the radial resolution, the "toroidal" field-of-view of this array has been reduced for future experiments.

Results - Local Emissivities

The measurements of the Side Arrays and the Top Array #1 have been combined and inverted without recourse to symmetry assumptions to yield local volume emission rates by a procedure described by Kurz, et al.[7] An example of a measured distribution of D_{α} emission is shown as Figure 1 of that reference. Measurements of C^{+2} (λ~465 nm) emission have also been made. For C^{+2}, data from only the Top Array #2 and the Side Array #1 are available from the last Alcator C-Mod run period. By choosing a time when the radial emission bands were less prominent (than in Fig. 2b for example), the chordal measurements have been inverted with the understanding that some of the radial structure will be washed out by the too-large field-of-view of Top Array #2. The result of such an inversion is shown in Figure 3. As expected for the diverted C-Mod discharges, the D_{α} and C^{+2} emissions are asymmetric poloidally and concentrated around the divertor.

Accurate measurement of these and similar emission structures was the goal of the configuration of the arrays and the inversion technique. These local emission rates allow determination of spatially resolved ionization rates and particle confinement times for H [ref. 2]., and are being used to determine local influxes of C^{+2} [ref. 8].

Acknowledgement

This work was supported by U.S. DOE Contract No. DE-AC02-78ET51013.

References

[1] P.C. Stangeby, Nucl. Fus. 33,1695 (1994).

[2] L.C. Johnson, E. Hinnov, J. Quant. Spectrosc. Radiative Transfer **13**, 333 (1973).

[3] W.L. Rowan, C.C. Klepper, C.P. Ritz, R.D. Bengston, et al., Nucl. Fus. **27**, 1105 (1987).

[4] I.H. Hutchinson, R. Boivin, F. Bombarda. P.Bonoli, et al., Physics of Plasmas **1** , 1511 (1994)

[5] S. Von Goeler, W. Stodiek and N. Sautoff, PRL **33**, 1201 (1974).

[6] Product sold by EG & G Reticon, Salem, MA 01970

[7] C. Kurz, J.L. Terry, J.A. Snipes, "Determination of H_α Emissivities from Line-Integrated Brightness Measurements on Alcator C-Mod", Rev. Sci. Instrum., these proceedings.

[8] C. Kurz, B. Lipschultz, G. McCracken, M. Graf, et al., Proc. 11th International Conf. in Plasma Surface Interactions, Mito, Japan (1994), J. Nucl. Mater., to be published.

Figure Captions

Figure 1. The cross-section of the C-Mod vacuum vessel, including the fields-of-view of the 4 visible arrays. Some of the views are displaced toroidally.

Figure 2. (a) The D_α chord brightness profile constructed from the two arrays which view the discharge from the side. The chord at a height of -0.48 m views the inner nose of the divertor (the line labeled 'α'). (b) The D_α chord brightness profile constructed from the two arrays which view the discharge from above. The chord intersecting a midplane major radius at 0.621 m views the inner nose of the divertor (the line labeled 'β'), while the chord intersecting at 0.684 m views the outer nose (the line labeled 'γ'). There are 60 chordal measurements from each of the side arrays and Top Array #2. There are 35 chordal measurements from Top Array #1.

Figure 3. The profile of C^{+2} (λ~465 nm) emission 0.25 s after plasma initiation. The plasma has just become diverted at this time. Also shown are the grid of 5x5 cm^2 pixels used for the inversion, the separatrix, and the gray scale for the emission rate (at left). Although there is only one value of emission per pixel, the inverted data have been smoothed, leading to the appearance of structure finer than the grid.

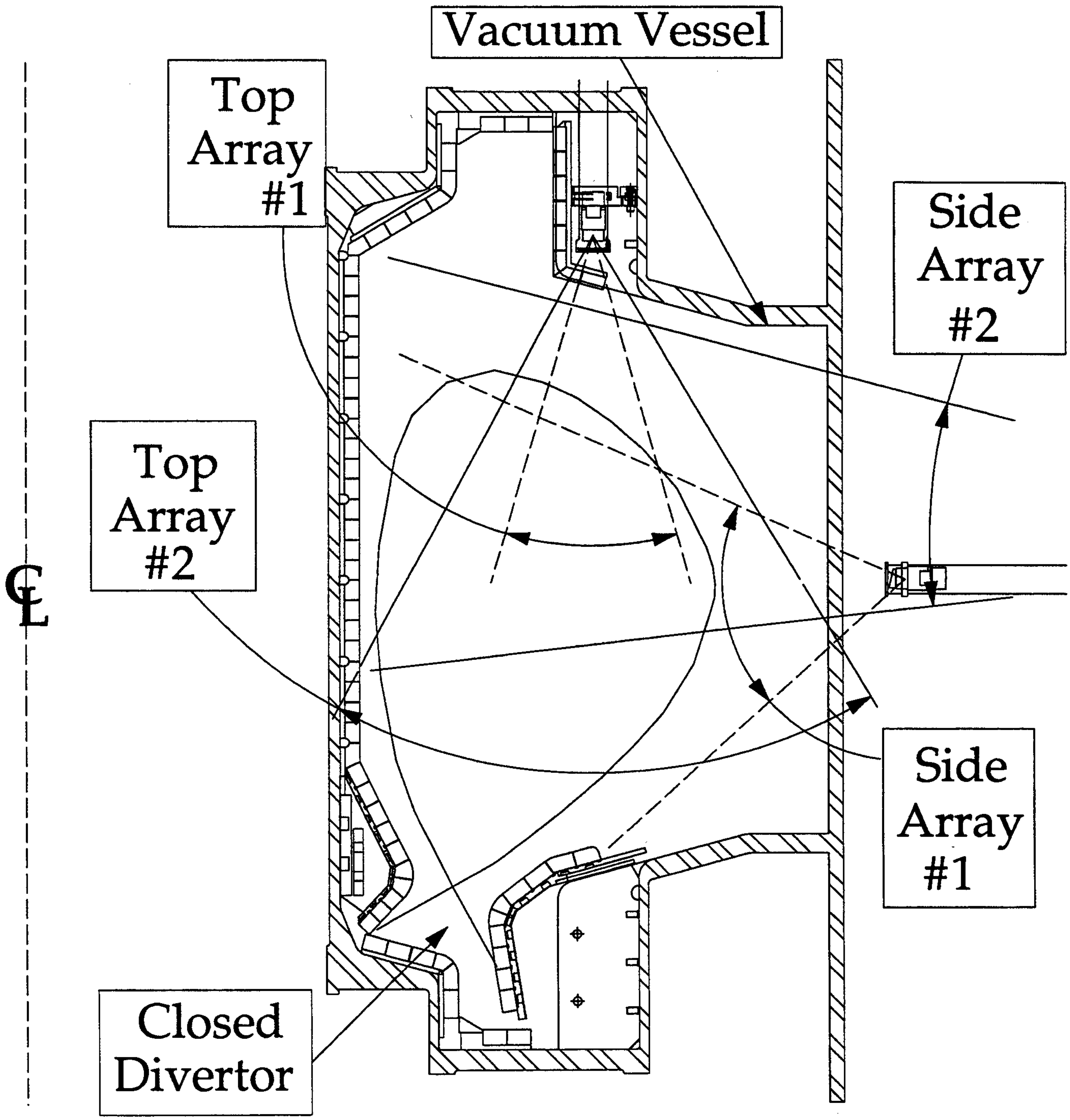

Vacuum Vessel
Top Array #1
Side Array #2
Top Array #2
℄
Side Array #1
Closed Divertor

Figure 1

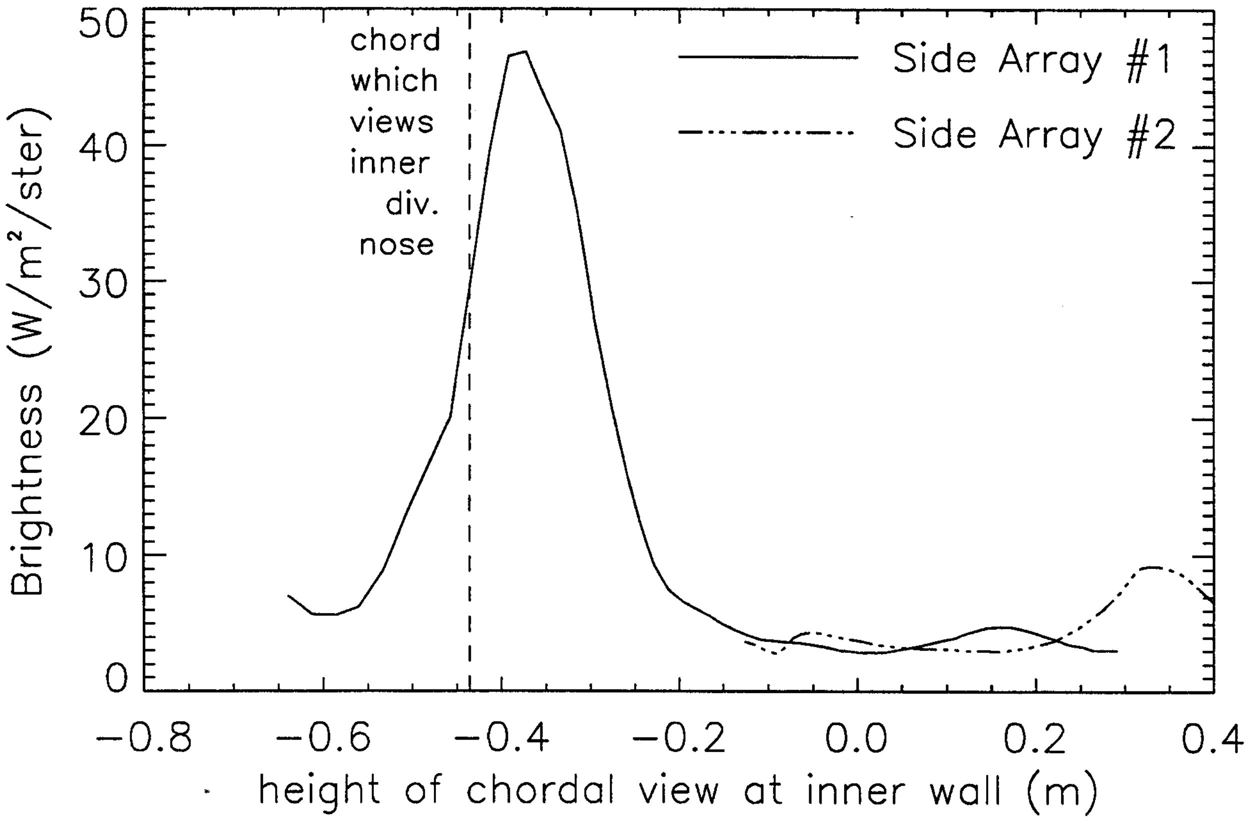

Figure 2(a)

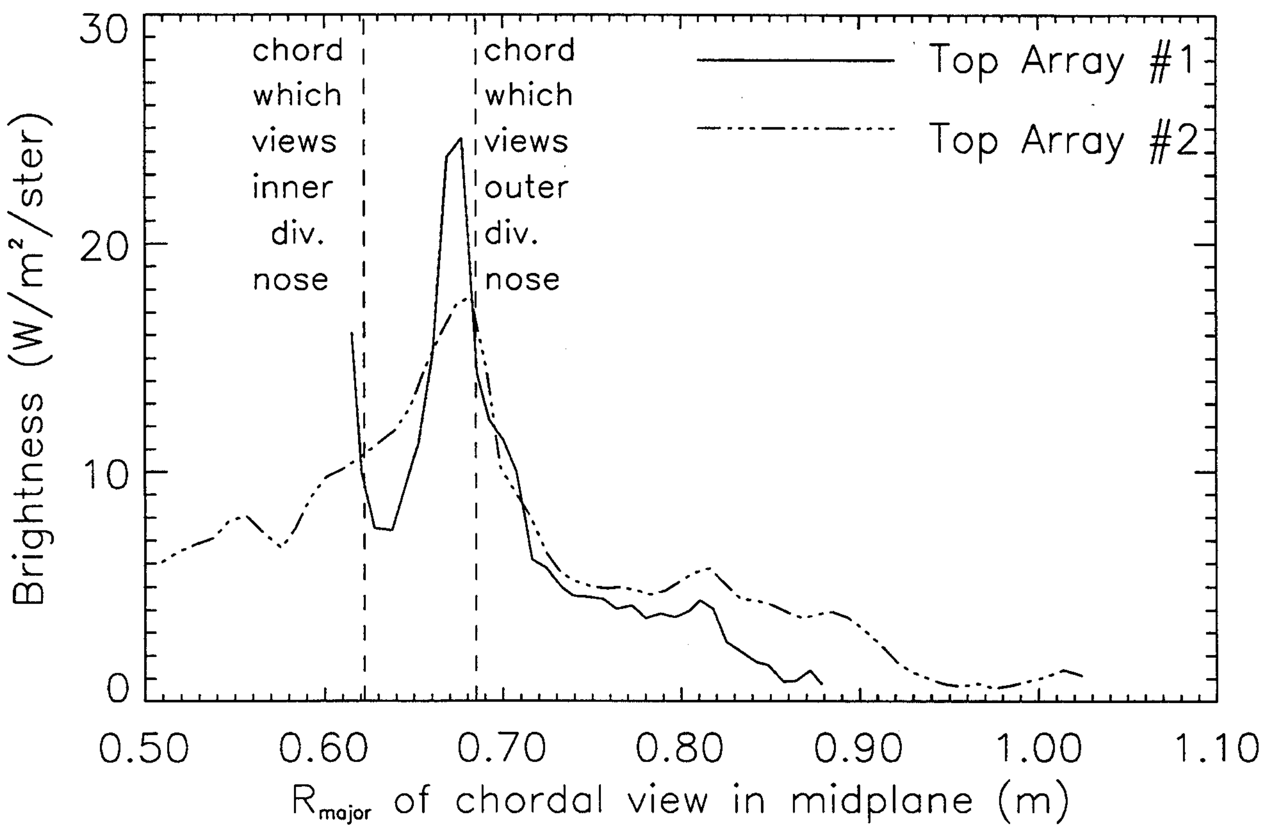

Figure 2(b)

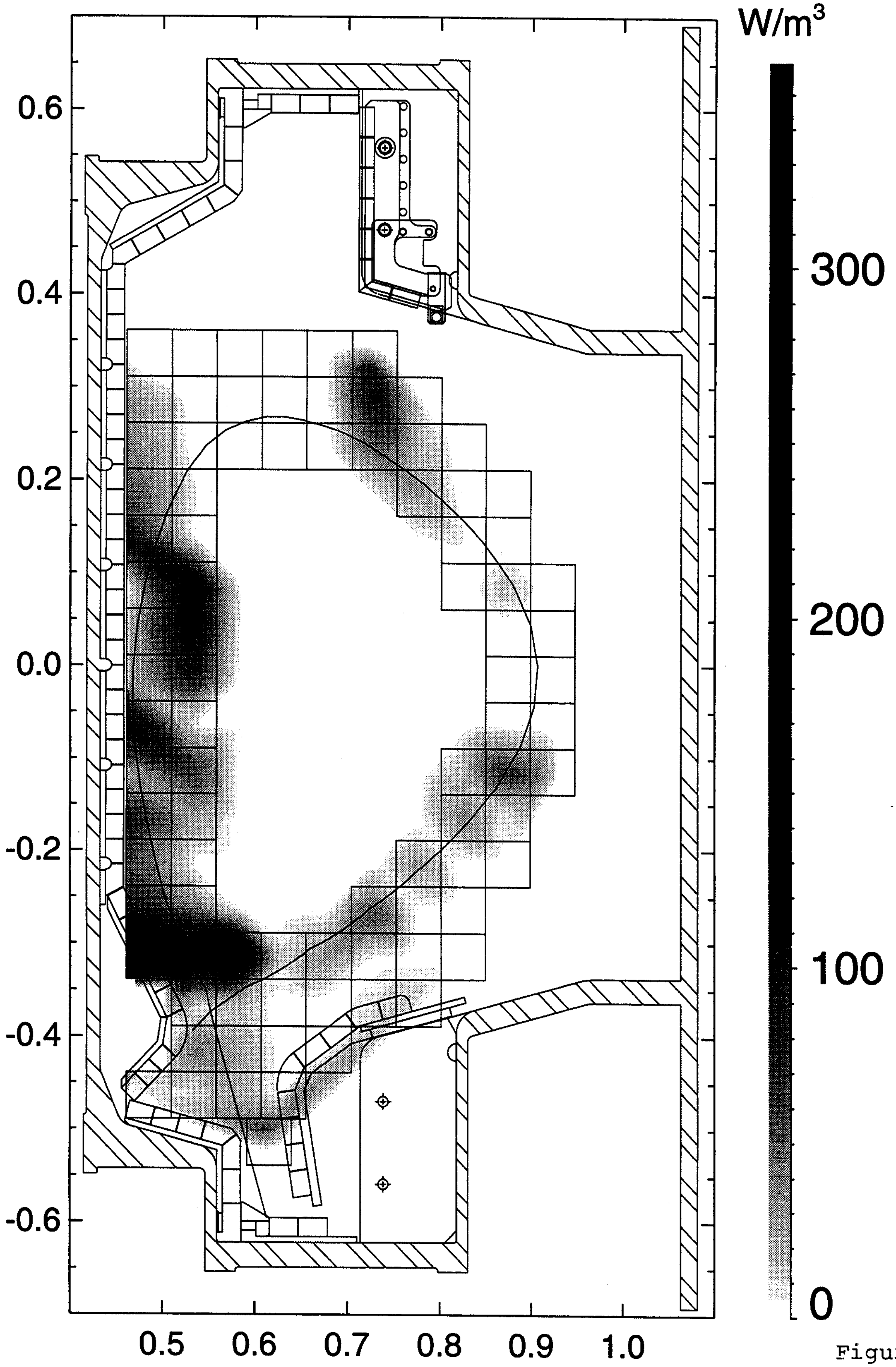

Figure 3